Theory of Hyperfine Properties of Beryllium and Magnesium Metals*

P. JENA† AND T. P. DAS†
Department of Physics, University of California, Riverside, California 92507

AND

S. D. MAHANTI
Bell Telephone Laboratories, Murray Hill, New Jersey 07974

(Received 25 May 1969)

A detailed analysis of the hyperfine properties of the lighter group-II metals, beryllium and magnesium, has been carried out to understand the relation between the electronic structures of these hcp metals. The "lens" and "butterflies" of the magnesium Fermi surface have large s character, leading to an appreciable value of the Knight shift K_s. In contrast, beryllium does not have these pieces of the Fermi surface, and this qualitatively explains the vanishingly small K_s for beryllium. Core polarization (cp) plays an important role in explaining the experimental values of K_s. There is a basic difference between beryllium and magnesium as regards the cp contribution to the Knight shift (K_{cp}). For beryllium, $K_s^{cp,p}$, the p part of the cp contribution is negative and this, together with a small direct contribution K_s^d, leads to a vanishingly small value for K_s ($0.7\times10^{-3}\%$), as compared to $-0.25\times10^{-2}\%$ obtained experimentally. Orbital effects are expected to explain the remaining discrepancy in beryllium. For magnesium, K_s^{cp} is roughly 38% of K_s^d, and the total theoretical value of K_s is 0.0554%, compared to the experimental value of 0.112%. The uncertainties in the exchange enhancement of χ_p and the role of other contributions to K_s are discussed. The relaxation time in beryllium is quite large because of the small spin density, and T_1T is found to be 1.0035×10^4 deg sec as compared to 1.66×10^4 obtained experimentally. No experimental value of T_1T is available for magnesium. Our theoretical value, including exchange enhancement effects, is 0.0346 $\times10^4$ deg sec. The relatively large p contribution to K_s^{cp} in both the metals plays an important role in the deviation of $K_s^2T_1T$ from its ideal value, $(\gamma_e/\gamma_N)^2\hbar/4\pi k_B$.

I. INTRODUCTION

THE first-principle theoretical interpretation of hyperfine properties of metals available from resonance experiments provides a detailed test of our knowledge of electronic wave functions. These properties provide information on electronic behavior in position space, in the same way that cyclotron resonance, the de Haas–van Alphen effect, and associated properties provide information about momentum space, particularly in the vicinity of the Fermi surface. Among the hyperfine properties that are available from magnetic resonance experiments are the isotropic and anisotropic Knight shifts, the relaxation time, and the nuclear quadrupole coupling tensor.[1] The first three of these also require a detailed knowledge of the Fermi surface, since they depend on the spin susceptibility χ_p, and the wave functions of the conduction electrons at the Fermi surface. The metals in which hyperfine properties are understood in most quantitative detail are the alkali metals[2] whose electronic structure and Fermi surface are relatively simple. Detailed analyses[3] have also been performed in metallic lead, whose Fermi surface,[4–6] though complex, is well understood both theoretically and experimentally. The group-II metals are more complex than the alkali metals for two reasons. One is their hcp structure, in contrast to the cubic structure of alkali metals. Secondly, they have four electrons per unit cell which is enough to fill two Brillouin zones. The Fermi surfaces in these metals are thus expected to be of a more complicated nature than in the alkali metals. However, by a combination of detailed experimental and theoretical analyses, the band structure and Fermi surface of these metals are well understood. Three of the group-II metals in which resonance data are available are beryllium, magnesium, and cadmium. The c/a and m^*/m ratios in these metals (Table I), as well as in zinc, provide an interesting comparison among themselves. While the c/a ratios make beryllium and magnesium more similar to each other, with respect to the m^*/m ratio, magnesium is an exception compared to the other three. There seems, therefore, to be an interesting interplay between the lattice structure which determines the framework of the Brillouin zone and the potential experienced by the conduction electrons. With respect to the latter, beryllium and magnesium are expected to be more similar to each other and different from zinc and cadmium because the latter have d electrons in their outermost cores. The combination of these two factors characterizes the nature of the Fermi surface in each case. An analysis of the magnetic and hyperfine properties of these metals should therefore provide a better understanding of the relation between the electronic structures of these metals. In this paper, we present a detailed analysis of the direct and core-polarization[7] (cp)

* Work at Riverside supported by National Science Foundation.
† Present address: Department of Physics, University of Utah, Salt Lake City, Utah.
[1] C. P. Slichter, *Principles of Magnetic Resonance* (Harper and Row, Inc., New York, 1963).
[2] S. D. Mahanti and T. P. Das, Phys. Rev. **183**, 674 (1969).
[3] L. Tterlikkis, S. D. Mahanti, and T. P. Das, Phys. Rev. Letters **21**, 1796 (1968).
[4] J. R. Anderson and A. V. Gold, Phys. Rev. **139**, A1459 (1965).
[5] P. Soven, Phys. Rev. **137**, A1706 (1965).
[6] T. L. Loucks, Phys. Rev. **136**, 784 (1964).
[7] G. D. Gaspari, W. M. Shyu, and T. P. Das, Phys. Rev. **134**, A852 (1964).

TABLE I. Some structural, band, and electronic properties of group-II metals.

Metal	c/a	a	r_s	$(m^*/m)_{\text{expt}}$[a]	$(m^*/m)_{\text{theor}}$[b]	Electronic configuration
Beryllium	1.567	4.3211	2.37	0.45 0.37	0.45	$2s^2$
Magnesium	1.624	6.026	3.324	1.23 0.946	...	$2p^6\ 3s^2$
Zinc	1.828	5.0256	2.884	0.842 0.601	0.59	$3d^{10}\ 4s^2$
Cadmium	1.862	5.6092	3.239	0.731 0.515	0.54	$4d^{10}\ 5s^2$

[a] The upper values represent (m^*/m) obtained directly from specific-heat data [Be, Ref. 36; Mg, Ref. 28; Zn, G. Seidel and P. H. Keesom, Phys. Rev. **112**, 1083 (1958); Cd, N. E. Phillips, Phys. Rev. **134**, A385 (1964)] and the lower ones, after applying electron-phonon correction factors calculated by McMillan (Ref. 30) for Be, P. H. Allen, M. L. Cohen, L. M. Falicov, and R. V. Kasowski, Phys. Rev. Letters **21**, 1794 (1968) for Zn and Cd. For magnesium no such calculation is available. A 30% correction is used in comparison with Na and Al.
[b] The theoretical values are from band calculations; for Be, Ref. 13 (OPW procedure), and for Zn and Cd, Ref. 21 (pseudopotential procedure).

contributions to the isotropic Knight shift K_s and relaxation time T_1, in magnesium and beryllium. The Knight shift in beryllium has been reported[8] briefly earlier. We shall include more details of the beryllium calculation as well as an analysis of the relaxation time. A comparison of the results in the two metals provides a deeper insight into the mechanisms that are responsible for the contrasting experimental situations of a small negative Knight shift in beryllium and an appreciable positive shift in magnesium. A subsequent paper will report the results of our analysis on cadmium which are currently under progress. A comparison of the origin of χ_p and the hyperfine properties in all three hcp metals will be made there, to provide a broader knowledge of this entire group of metals.

Section II will deal with the direct contribution to the spin density from various parts of the Fermi surface and the averaging procedure utilized to get the total spin density. In Sec. III we will be concerned with the cp[7] contribution to spin density. The exchange enhancement effects on both spin susceptibility and relaxation rate will be discussed in Sec. IV. The results of our theoretical calculation of Knight shift, T_1 and the Korringa constant will be analyzed in Sec. V and compared with available experimental data. In Sec. VI, the conclusions from our investigations will be summarized and suggestions will be made for further research to obtain an improved understanding of the properties of these metals.

II. ANALYSIS OF SPIN DENSITY AT NUCLEUS

The direct contribution[1] $K_s{}^d$ to the Knight shift is given by

$$K_s{}^d=(8\pi/3)\chi_p{}^*\Omega_0\langle|\Psi_F(0)|^2\rangle_{\text{av}}{}^d\equiv(8\pi/3)\chi_p{}^*\Omega_0 S_d\,, \quad (1)$$

where $\chi_p{}^*$ is the spin susceptibility per unit volume (in cgs volume units), Ω_0 is the volume of the Wigner-Seitz cell over which the conduction electron wave function is normalized, and $\langle|\Psi_F(0)|^2\rangle_{\text{av}}{}^d$ is the averaged direct spin density at the nucleus due to the conduction electrons at the Fermi surface. The evaluation of $K_s{}^d$ from Eq. (1) requires a knowledge of the spin susceptibility and a detailed knowledge[8] of the hyperfine matrix elements at various points on the Fermi surface to carry out the average. In this section, the evaluation of the spin density using the calculated wave functions will be described. The calculation of the spin-susceptibility requires a consideration of the effects[9] of exchange and correlation among the conduction electrons, and will be discussed in Sec. IV.

We have utilized the orthogonalized-plane-wave[10] (OPW) model for obtaining the energy bands and wave functions required for our spin-density calculation. Since a number of reviews[11,12] of the OPW method are available, we shall only mention the basic steps of our calculation briefly, both to introduce our notations and to give an idea of the accuracy of our wave functions. The wave function of a Bloch electron in an OPW representation is given by

$$\Psi_{\mathbf{k}}(\mathbf{r})=\sum C(\mathbf{k}+\mathbf{K})\Psi_{\text{OPW}}(\mathbf{k}+\mathbf{K},\mathbf{r})\,, \quad (2)$$

the summation being carried over the reciprocal-lattice vectors $\mathbf{K}$, and a typical OPW function is expressed as

$$\Psi_{\text{OPW}}(\mathbf{k},\mathbf{r})=\Omega_0{}^{-1/2}e^{i(\mathbf{k})\cdot\mathbf{r}}-\sum_t B_t(\mathbf{k})\varphi_t(\mathbf{r})\,, \quad (3)$$

where t refers to the core states of the crystal, and $\varphi_t(\mathbf{r})$ is the core wave function. The orthogonalization parameters $B_t(\mathbf{k})$ are given by

$$B_t(\mathbf{k})=\Omega_0{}^{-1/2}\langle\varphi_t|e^{i\mathbf{k}\cdot\mathbf{r}}\rangle\,. \quad (4)$$

Using a spherical harmonic expansion for $e^{i\mathbf{k}\cdot\mathbf{r}}$ and replacing t by the quantum numbers nlm of the core states, we obtain

$$B_{nlm}(\mathbf{k})=4\pi(i)^l\Omega_0{}^{-1/2}Y_{lm}{}^*(\hat{k})T_{nl}(k)\,, \quad (5)$$

[8] P. Jena, S. D. Mahanti, and T. P. Das, Phys. Rev. Letters **20**, 544 (1968).
[9] S. D. Silverstein, Phys. Rev. **130**, 912 (1963).
[10] C. Herring, Phys. Rev. **57**, 1169 (1940).
[11] T. O. Woodruff, in *Solid State Physics*, edited by F. Seitz and D. Turnbull (Academic Press Inc., New York, 1957).
[12] J. Callaway, *Energy Band Theory* (Academic Press Inc., New York, 1964).

where

$$T_{nl}(k)=\int_0^\infty j_l(kr)U_{nl}(r)r\,dr. \tag{6}$$

Here $U_{nl}(r)$ is related to the atomic core function $\varphi_{nlm}(\mathbf{r})$ by the equation

$$\varphi_{nlm}(\mathbf{r})=[U_{nl}(r)/r]Y_{lm}(\theta,\varphi). \tag{7}$$

The coefficients $C(\mathbf{k}+\mathbf{K})$ are obtained variationally by solving the usual set of linear equations.

The lattice parameters for beryllium and magnesium that we have used in our calculation are given in Table I. For the core functions $\varphi_{nlm}(\mathbf{r})$, we have employed pseudocore wave functions for both beryllium[13] and magnesium[14] used by earlier workers. The potential for magnesium was obtained by Falicov[14] in an earlier band-structure calculation.

The band structure of beryllium[13,15,16] has been analyzed theoretically by several first-principle calculations which give good agreement with experimental Fermi-surface[17] data from de Haas–van Alphen measurements. We have employed in our calculation for this metal the potential tabulated by Loucks and Cutler.[13] For both beryllium and magnesium, the number of basis functions employed in constructing the linear combination of OPW's (LCOPW) was about 23. The exact number varied between 22 and 24, depending on the location of the point $\mathbf{k}$ in the Brillouin zone (Fig. 1). Since most of the points on the Fermi surface that we considered were not points of high symmetry, group theoretic factorization of the secular equations was not particularly helpful and was not used.

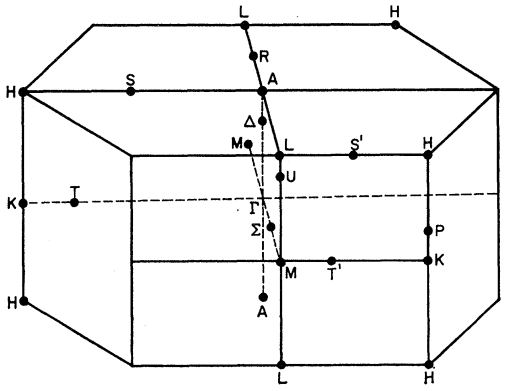

FIG. 1. First Brillouin zone for the hexagonal close-packed structure. The ΓA, ΓM, and ΓK directions correspond to the [0001], [10$\bar{1}$0], and [11$\bar{2}$0] crystallographic directions, respectively.

The Fermi surfaces of beryllium[13] and magnesium[14,18–20] are made up of a number of segments which are given descriptive names for the sake of visualization. In the case of magnesium, there are two very small identical hole pockets in the first zone, referred to as *caps* [Fig. 2(b)]; a large multiply connected hole surface in the second zone, which contributes the major part of the area of the Fermi surface and is referred to as the *monster* [Fig. 2(a)]; two identical electron pockets in the third zone with triangular cross sections, resembling *cigars* [Fig. 2(c)]; a large electron pocket in the third zone centered on Γ, which is referred to as a *lens* [Fig. 2(d)]; and three identical electron pockets in the third zone around L, referred to as *butterflies* [Fig. 2(e)]. The Fermi surface of beryllium[13] is somewhat simpler by comparison, containing only two segments: a large hole surface in the second band, which is referred to as a *coronet* and is the counterpart of the monster in magnesium, and two identical pockets of electrons in the third zone referred to as cigars. The cigars in beryllium are much more pronounced than those in magnesium and constitute the entire electron part of the Fermi surface. In addition to these differences in the nature of the segments of the Fermi surfaces for the two metals, the features of the Fermi surface in magnesium are found to be reasonably well reproduced by the Harrison[21] one-OPW model. In beryllium, on the other hand, the resemblance between the result of Harrison construction and the actual Fermi surface is poor. In particular, the former predicts[21] a lens and butterflies as in magnesium, but these are absent in the actual Fermi surface of beryllium.[13,17] A consequence of this difference in the nature of the Fermi surface of these two metals is the difference in their effective masses m^*, magnesium being more free-electron-like. The difference in the features of the Fermi surfaces in the two metals will have a bearing on the spin density at the nuclei as we shall see presently.

The Knight shift expression (1) requires an evaluation of the average over the Fermi surface of $|\Psi_F(0)|^2$ due to electrons at the Fermi surface. To carry out this average, one requires a knowledge of the local density of states at points (j) on the surface (ith segment)

$$g_{ij}(\mathbf{k}_F)=|\nabla_k E_{ij}|_{E_{ij}=E_F}{}^{-1}. \tag{8}$$

The Fermi surface average is obtained by combining the averages over the different segments of the Fermi surface. Thus $\langle|\Psi_F(0)|^2\rangle_i$, the average spin density for the ith segment, is given by

$$\langle|\Psi_F(0)|^2\rangle_i=\textstyle\sum_j g_{ij}(\mathbf{k}_F)\,|\Psi_F(0)|_{ij}{}^2/\sum_j g_{ij}(\mathbf{k}_F), \tag{9}$$

where the summation on j runs over points on the segment i. In our calculation we have chosen points on

[13] T. L. Loucks and P. H. Cutler, Phys. Rev. **133**, A819 (1964); T. L. Loucks, *ibid.* **134**, A1618 (1964).
[14] L. M. Falicov, Phil. Trans. Roy. Soc. London **A255**, 55 (1962). We are grateful to Professor Falicov for kindly supplying us with the pseudocore wave functions.
[15] J. H. Terrel, Phys. Rev. **149**, 526 (1966).
[16] C. Herring and A. G. Hill, Phys. Rev. **58**, 132 (1954).
[17] B. R. Watts, Phys. Letters **3**, 284 (1963).
[18] J. C. Kimball, R. W. Stark, and F. M. Mueller, Phys. Rev. **162**, 600 (1967).
[19] J. B. Ketterson and R. W. Stark, Phys. Rev. **156**, 748 (1967).
[20] R. W. Stark, Phys. Rev. **136**, A998 (1964).
[21] W. A. Harrison, *Pseudo-potential in Theory of Metals* (W. A. Benjamin, Inc., New York, 1966).

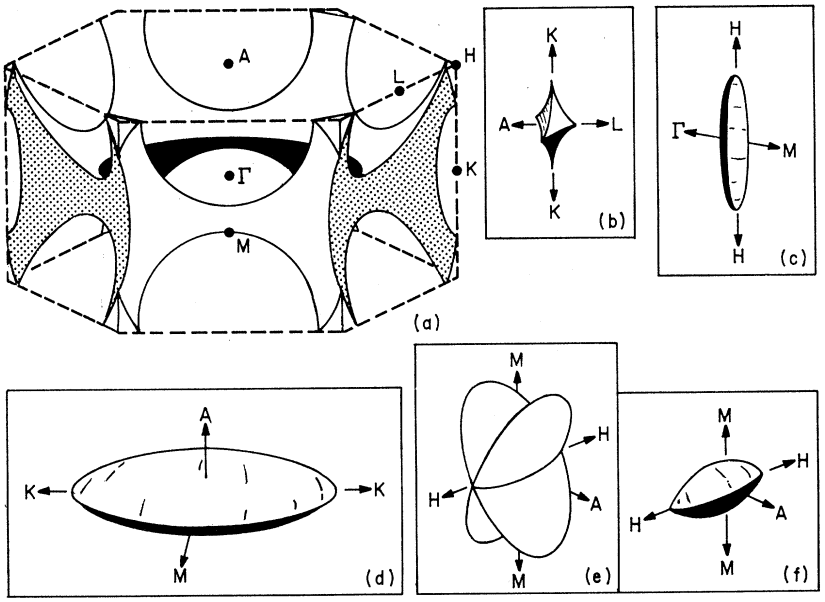

FIG. 2. Single-OPW Fermi surfaces of magnesium: (a) monster (second-zone holes); (b) cap (first-zone holes); (c) cigar (third-zone electrons); (d) lens (third-zone electrons); (e) butterfly (third-zone electrons); (f) (fourth-zone electrons).

symmetry lines and symmetry planes and utilized proper geometrical factors to include the contributions from equivalent points to the summation (9). A comparison of the average spin densities $\langle|\Psi_F(0)|^2\rangle_i$ reveals the relative extent of s character for the different segments of the Fermi surface, since the non-s parts of the wave functions do not contribute to the direct spin density at the nucleus. The contributions from all the segments are then combined as in Eq. (10) to obtain the average over the entire Fermi surface.

$$\langle|\Psi_F(0)|^2\rangle_{\rm av}=\sum_i S_i\langle|\Psi_F(0)|^2\rangle_i/\sum_i S_i. \qquad (10)$$

In Eq. (10), S_i is the surface area of the ith segment of the Fermi surface.

The direct spin densities $|\Psi_F(0)|_d^2$ at various points on the Fermi surface, chosen in our calculation, are listed in Table II. This table also includes the density-of-states function $g_{ij}(\mathbf{k}_F)$ and cp contributions to the spin density, to be discussed in Sec. III. The corresponding results for $|\Psi_F(0)|_d^2$ in beryllium have been presented earlier[8] and will not be repeated here. The net contributions to the direct spin density are included in Tables III and IV for beryllium and magnesium.

In beryllium, the direct spin-density results indicate that the cigars have more s character than the coronet. However, the contributions of both of these segments to the direct spin density are small. In magnesium, we see from Table II that the lens and butterflies which are absent in beryllium, have strong s character and the direct spin density in magnesium is, therefore, much larger than in beryllium. The cigars are more s-like than the monster, a feature similar to beryllium. The contribution from the cigars is, however, much smaller than that from the lens and butterflies, since the cigars have very little surface area in magnesium. The surface areas that are needed in Eq. (10) to obtain the net

TABLE II. Direct and cp contributions to the spin density (S_d,$S_{\rm cp}$) from various points on the Fermi surface of magnesium.

Coordinate	Segment	S_d	$S_{\rm cp}{}^s$	$S_{\rm cp}{}^p$	$S_{\rm cp}{}^d$	$1/\lvert\nabla_k E\rvert$
(0, 0, 0.058)		0.6858	0.1543	0.0161	−0.0038	0.9346
(0.2208, 0.1275, 0)	Lens	0.6303	0.1554	0.0311	−0.0030	7.6923
(0.253, 0, 0)		0.6427	0.1492	0.0274	−0.0032	2.5270
(0.6951, 0, 0.2771)		0.0220	0.0022	0.0700	−0.0014	1.6284
(0.6211, 0, 0)	Cigars	0.2047	0.0637	0.0605	−0.0021	1.2484
(0.6731, 0.0381, 0)		0.2999	0.0815	0.0556	−0.0019	0.1792
(0.5213, 0.301, 0.2921)		0.7161	0.1910	0.0110	−0.0044	3.8461
(0.5213, 0.301, 0.2711)	Butterflies	0.6771	0.1858	0.0120	−0.0045	3.8097
(0.5022, 0.29, 0.3211)		0.6891	0.1556	0.0184	−0.0045	2.1157
(0.5428, 0.2638, 0.3211)		0.7200	0.1678	0.0136	−0.0044	4.3643
(0.6891, 0.0104, 0.3211)		0.0011	0.0070	0.0732	−0.0012	1.4762
(0.606, 0, 0)		0.1736	0.0429	0.0528	−0.0022	1.1864
(0.405, 0, 0)	Monster	0.0	0.0	0.0576	−0.0016	1.2456
(0.3914, 0.226, 0)		0.0701	0.0155	0.0586	−0.0018	1.1205
(0.3594, 0.2075, 0)		0.0602	0.0124	0.0631	−0.0020	1.1467

TABLE III. Direct and cp contributions to the spin density (S_d and S_{cp}) from various segments of the Fermi surface of beryllium.

Segments of Fermi surface	$S_d\times10^2$	$S_{cp}{}^s\times10^2$	$S_{cp}{}^p\times10^2$	$S_{cp}{}^d\times10^2$	$S_{tot}\times10^2$
Coronet	2.0871	0.3767	−1.8110	−0.0878	0.5651
Cigar	8.0210	1.5348	−2.3162	−0.1263	7.0341
Total	10.1081	1.9115	−4.1272	−0.2141	7.5992

Fermi surface average are tabulated for magnesium in Table IV. The areas from experimental dimensions agree very well with those from the Harrison construction[21] for the cigar. For the other three segments there are sizable differences reflecting the influence of the potential. Since the band-structure[14,18] calculation gives linear dimensions and cross sections in good agreement with experiment,[19,22] it is fair to say that the former would also give surface areas in reasonable agreement with the experiment. For beryllium, a similar comparison with Harrison construction[21] is not meaningful. The surface areas of cigars and coronet are obtained from Loucks and Cutlers'[13] band calculation. The direct spin densities averaged over the entire Fermi surface [S_d of Eq. (1)] were found by this procedure to be

$$S_d{}^{Mg}=0.2409 \tag{11}$$

for magnesium, and

$$S_d{}^{Be}=0.1011 \tag{12}$$

for beryllium.

It is more meaningful to compare the ratios of these densities to that of the valence s states ($2s$ for beryllium and $3s$ for magnesium) in the corresponding atoms. Since the atomic hyperfine effect is measured in the ^3P state, one should use the valence s-state function in this atomic state. However, the valence s function does not vary very much between the $^1S(3s^2)$ and the $^3P(3s3p)$ states and so we have used the former for comparison. One then gets

$$S_d{}^{Mg}/|\varphi_{3s}(0)|_{Mg}{}^2=0.2185, \tag{13}$$

$$S_d{}^{Be}/|\varphi_{2s}(0)|_{Be}{}^2=0.1340. \tag{14}$$

These ratios clearly demonstrate the larger fractional s character in magnesium metal. This fact, coupled with the difference in the nature of the cp in the two metals, to be discussed in Sec. III, provides an explanation of the contrasting situations for K_s in these two metals.

A knowledge of the average wave function densities in Eqs. (11) and (12) also allows an evaluation of the direct contribution to spin-lattice relaxation time (T_1). The expression for the direct contribution to $T_1{}^{-1}$ is given by

$$(T_1T)_d{}^{-1}=A(S_d)^2, \tag{15}$$

where $A=(16\pi/9)\hbar^3\gamma_e{}^2\gamma_N{}^2k_Bg^2(E_F)\Omega_0{}^2$, $g(E_F)$ is the density of states per electron (instead of the density per spin state, which is smaller by a factor of $\frac{1}{2}$) at the Fermi surface, and where k_B is the Boltzmann constant. On substituting the result of Eqs. (11) and (12) for beryllium and magnesium in Eq. (15), we get

$$(T_1T)_d{}^{Mg}=0.85\times10^3 \text{ deg sec}, \tag{16}$$

$$(T_1T)_d{}^{Be}=1.4747\times10^4 \text{ deg sec}. \tag{17}$$

These values are obtained without the inclusion of correlation and exchange effects among the conduction electrons. The correction due to such effects and the additional contributions from cp effects will be considered in Secs. III and IV.

It should be noted that if exchange enhancement and cp effects are neglected for both K_s and $(T_1T)^{-1}$, then the Korringa constant[23] $K_s{}^2T_1T\gamma_N{}^2$ has the universal value

$$(K_s{}^2T_1T\gamma_N{}^2)=(\hbar/4\pi k_B)\gamma_e{}^2=1.88\times10^2. \tag{18}$$

The departure of the actual Korringa constant[23] from this result also reflects the relative importance of the above-mentioned effects and will be analyzed in Sec. V.

III. CP CONTRIBUTION TO SPIN DENSITY

In this section we shall be concerned with the additional spin density that arises at the nuclear site from the exchange polarization of core electrons in the presence of a magnetic field. Since the conduction electrons have a surplus spin polarization in a direction antiparallel to the magnetic field, the core electrons with spin antiparallel to the magnetic field will experience a different exchange potential due to the conduction electrons than those with opposite spins. The procedure for the calculation of the spin density and Knight shift due to this cp effect by the moment perturbed (mp) method have been described in a number of earlier papers.[7,24] This method amounts to calculating the magnetic moment induced in the core electrons through the magnetic hyperfine interaction and the interaction between this induced moment and the conduction electrons through the exchange effect. Since the steps involved in the calculation have been described in detail elsewhere[7] we shall merely quote the final expressions that are used for the actual quantitative evaluation. Thus, the spin density due to cp[7] is given by

$$S_{cp}=2\,\mathrm{Re}\sum_t(\langle\delta\varphi_t|\mathcal{H}_E|\varphi_t\rangle - \sum_{t'\neq t}\langle\delta\varphi_t|\varphi_{t'}\rangle\langle\varphi_{t'}|\mathcal{H}_E|\varphi_t\rangle)_{av}, \tag{19}$$

where the summations on t and t' extend over all the

[22] E. Fawcett, J. Phys. Chem. Solids 4, 320 (1961).

[23] J. Korringa, Physica 16, 601 (1950).

[24] W. M. Shyu, G. D. Gaspari, and T. P. Das, Phys. Rev. 141, 603 (1966); W. M. Shyu, T. P. Das, and G. D. Gaspari, *ibid.* 152, 270 (1966).

TABLE IV. Direct and cp contribution to the spin density from various segments of the Fermi surface of magnesium.

Segment of Fermi surface	Expt surface area of the segment	Surface area of the segment from Harrison construction	S_d	$S_{cp}{}^s$	$S_{cp}{}^p$	$S_c{}^d$	S_{tot}
Lens	0.6366	0.7804	0.6377	0.1543	0.0290	−0.0031	0.8179
Cigars	0.6252	0.6252	0.0813	0.0217	0.0669	−0.0016	0.1683
Butterflies	1.3452	2.4684	0.7050	0.1730	0.0138	−0.0044	0.8874
Monster	3.9996	2.7342	0.0466	0.0135	0.0638	−0.0016	0.1223

core states. The cp contribution to K_s is obtained by multiplying S_{cp} with $(8\pi/3)\chi_p{}^*\Omega_0$, the same factor that one uses to multiply S_d to get the direct Knight shift. In Eq. (19) the operator $\mathcal{H}_E$ describes the exchange between the core and conduction electrons and is given by

$$\mathcal{H}_E=\sum_i \mathcal{H}(i)=\sum_i \sum_k \alpha_{ik}(i)\,, \tag{20}$$

where

$$\alpha_{ik}(i)\,\varphi_i(\mathbf{r}_i)=\left(\int \Psi_k(\mathbf{r}_k)\frac{e^2}{r_{ik}}\varphi_i(\mathbf{r}_k)\,d\tau_k\right)\Psi_k(\mathbf{r}_i)\,. \tag{21}$$

The summation in "i" extends over all the core states and the summation in $\mathbf{k}$ over the conduction-electron states at the Fermi surface. The average in Eq. (19) is taken over the Fermi surface and $\delta\varphi_t$ are the mp functions corresponding to the core state φ_t. The $\delta\varphi_t$ are obtained by solving the perturbation equation

$$\left(-\nabla^2+\frac{\nabla^2\varphi_{ns}}{\varphi_{ns}}\right)\delta\varphi_{ns,N}$$
$$=-H_N\varphi_{ns}+\sum_{n's}\langle\varphi_{n's}|H_N|\varphi_{ns}\rangle\varphi_{n's}$$
$$+\sum_{n's}(\epsilon_{n's}-\epsilon_{ns})\langle\varphi_{n's}|\delta\varphi_{ns,N}\rangle\varphi_{n's}\,, \tag{22}$$

where φ_{ns} are core s functions and ϵ_{ns}, the corresponding eigenvalues and H_N is the Fermi contact term. The terms $t'\neq t$ in Eq. (19) arise out of nonorthogonality effects[25,26] involving the perturbed wave functions for the various cores. These terms do not occur for beryllium since it has only one core. On the other hand, in magnesium the equations for both $\delta\varphi_{1s}$ and $\delta\varphi_{2s}$ involve nonorthogonality terms between perturbed $1s$ and $2s$ core states. The radial equations corresponding to Eq. (22) for the magnesium $1s$ and $2s$ states are exactly identical in form to those for aluminum[24] and will not be reproduced here. The corresponding equation for the beryllium $1s$ core state has also been given earlier. The solution of the integrodifferential equation was carried out by a noniterative procedure to obtain the perturbed functions. For detailed analysis of the cp contribution to K_s and T_1, it is useful to separate S_{cp} into contributions from $s, p, d, \ldots$ parts of the conduction-electron wave function. The orthogonality of the spherical harmonics ensures that there are no cross terms such as $(sp), (pd), (sd), \ldots$ arising from cross interaction between the various angular momentum components. The following general expression applies to the contribution from the lth angular momentum component of the conduction-electron wave function:

$$S_{cp}{}^l=S_{cp}{}^l(\mathrm{I})+S_{cp}{}^l(\mathrm{II})\,, \tag{23}$$

$$S_{cp}{}^l(\mathrm{I})=2\,\mathrm{Re}\sum_n\Bigg[-\frac{4\pi}{\Omega_0}\sum_{\mathbf{K},\mathbf{K}'}C^*(\mathbf{k}+\mathbf{K}')C(\mathbf{k}+\mathbf{K})$$
$$\times P_l(\cos\theta_{\mathbf{k}+\mathbf{K}',\mathbf{k}+\mathbf{K}})\int_0^\infty \delta U_{ns}(r_1)$$
$$\times R_l(|\mathbf{k}+\mathbf{K}|,r_1)\,dr_1\left(\frac{1}{r_1{}^{l+1}}\int_0^{r_1}U_{ns}(r_2)r_2{}^l\right.$$
$$\times R_l(|\mathbf{k}+\mathbf{K}'|,r_2)\,dr_2+r_1{}^l\int_{r_1}^\infty U_{ns}(r_2)\frac{1}{r_2{}^{l+1}}$$
$$\left.\times R_l(|\mathbf{k}+\mathbf{K}'|,r_2)\,dr_2\right)\Bigg], \tag{24}$$

and

$$S_{cp}{}^l(\mathrm{II})=-2\,\mathrm{Re}\sum_{n\neq n'}\int_0^\infty \delta U_{ns}(r)U_{n's}(r)dr$$
$$\times\Bigg[-\frac{4\pi}{\Omega_0}\sum_{\mathbf{K},\mathbf{K}'}C^*(\mathbf{k}+\mathbf{K}')C(\mathbf{k}+\mathbf{K})$$
$$\times P_l(\cos\theta_{\mathbf{k}+\mathbf{K}',\mathbf{k}+\mathbf{K}})\left(\frac{1}{r_1{}^{l+1}}\int_0^{r_1}U_{ns}(r_2)r_2{}^l\right.$$
$$\times R_l(|\mathbf{k}+\mathbf{K}|,r_2)\,dr_2+r_1{}^l\int_{r_1}^\infty U_{ns}(r_2)\frac{1}{r_2{}^{l+1}}$$
$$\left.\times R_l(|\mathbf{k}+\mathbf{K}'|,r_2)\,dr_2\right)\Bigg], \tag{25}$$

with

$$R_l(|\mathbf{k}+\mathbf{K}|,r)$$
$$=rj_l(|\mathbf{k}+\mathbf{K}|r)-\textstyle\sum_n T_{nl}(|\mathbf{k}+\mathbf{K}|)U_{nl}(r)\,. \tag{26}$$

[25] K. J. Duff and T. P. Das, Phys. Rev. **168**, 43 (1968).
[26] A. Dalgarno, Proc. Roy. Soc. (London) **A251**, 282 (1959).

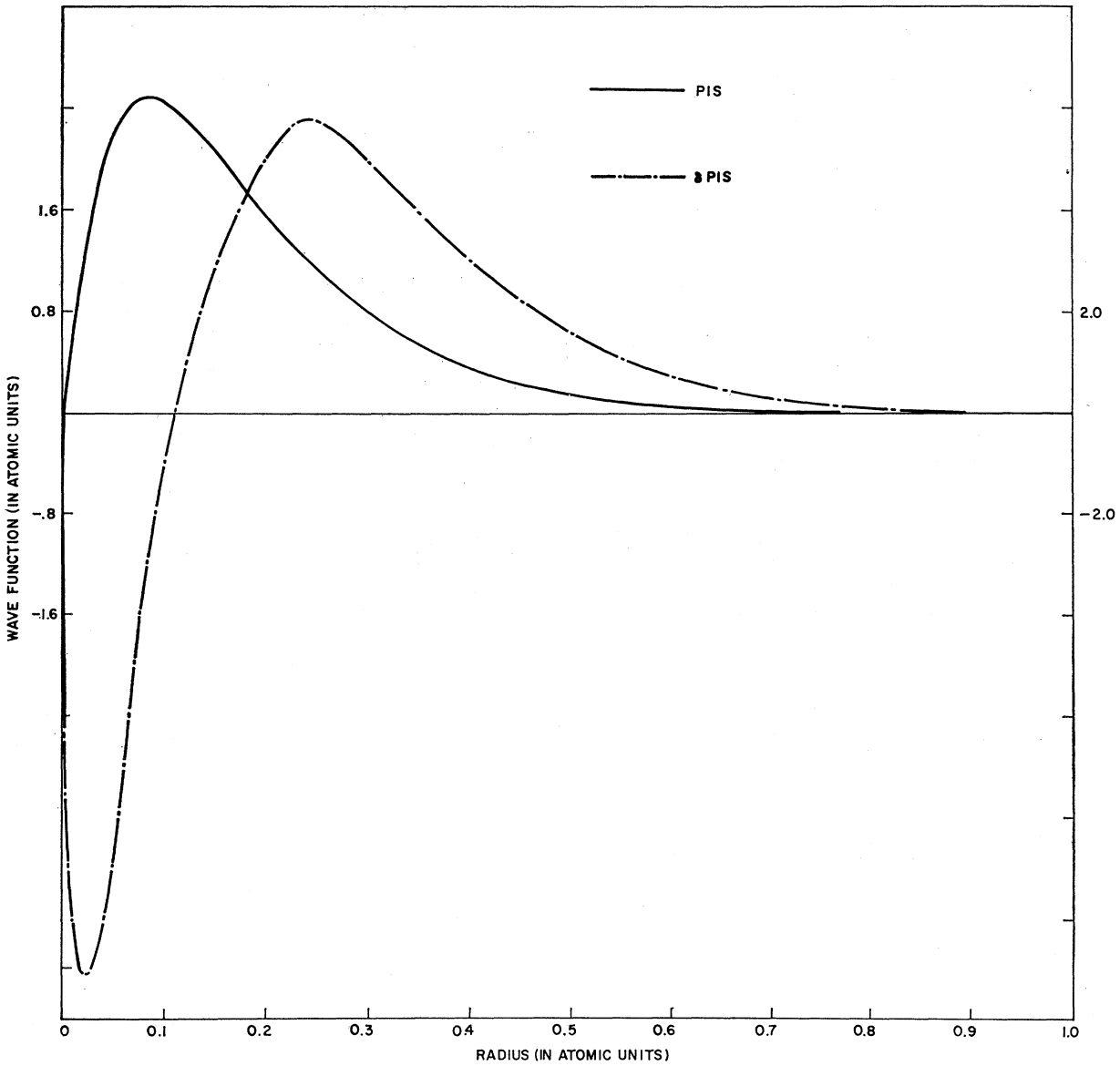

FIG. 3. Unperturbed P_{1s} and moment perturbed δP_{1s} states for magnesium. (Referred to as U_{1s} and δU_{1s} in the text.)

In Eqs. (24) and (25), the sums on n and n' run over all the core s states; but in Eq. (26), n refers only to the occupied core states of the particular angular momentum in question. The various contributions of $s, p, d, \ldots$ type are obtained by introducing $l=0, 1, 2, \ldots$ in Eqs. (24)–(26).

A plot of the mp function δU_{1s} for beryllium[24] is already available in the literature. We shall present only the functions δU_{1s} (Fig. 3) and δU_{2s} (Fig. 4) for magnesium. In addition to their use here, they could be helpful in the interpretations of Knight shift in magnesium alloys. To help in the understanding of the relative contributions from the polarizations of the $1s$ and $2s$ cores and from the s and p parts of the conduction-electron wave function (Ψ_{cond}), to be discussed later in the section, we have also presented the unperturbed atomic functions U_{1s}, U_{2s}, and U_{2p} in the same graphs. As in the analogous case of aluminum, δU_{1s} and δU_{2s} are seen to have one and two nodes, respectively. Using these mp functions and the expression for S_{cp} in Eq. (19), the contributions $S_{\text{cp}}{}^s$, $S_{\text{cp}}{}^p$, and $S_{\text{cp}}{}^d$ were calculated for magnesium. The nonorthogonality terms in S_{cp} in Eq. (19) involving the perturbed $1s$ and $2s$ functions gave mutually canceling contributions. Their sum total amounted to a small percentage (6%) of the direct term $S_{\text{cp}}(\text{I})$ similar to the situations for alkali metals and aluminum.[24] Further, as in these earlier cases, the ratio of the nonorthogonality[25,26] term to the direct

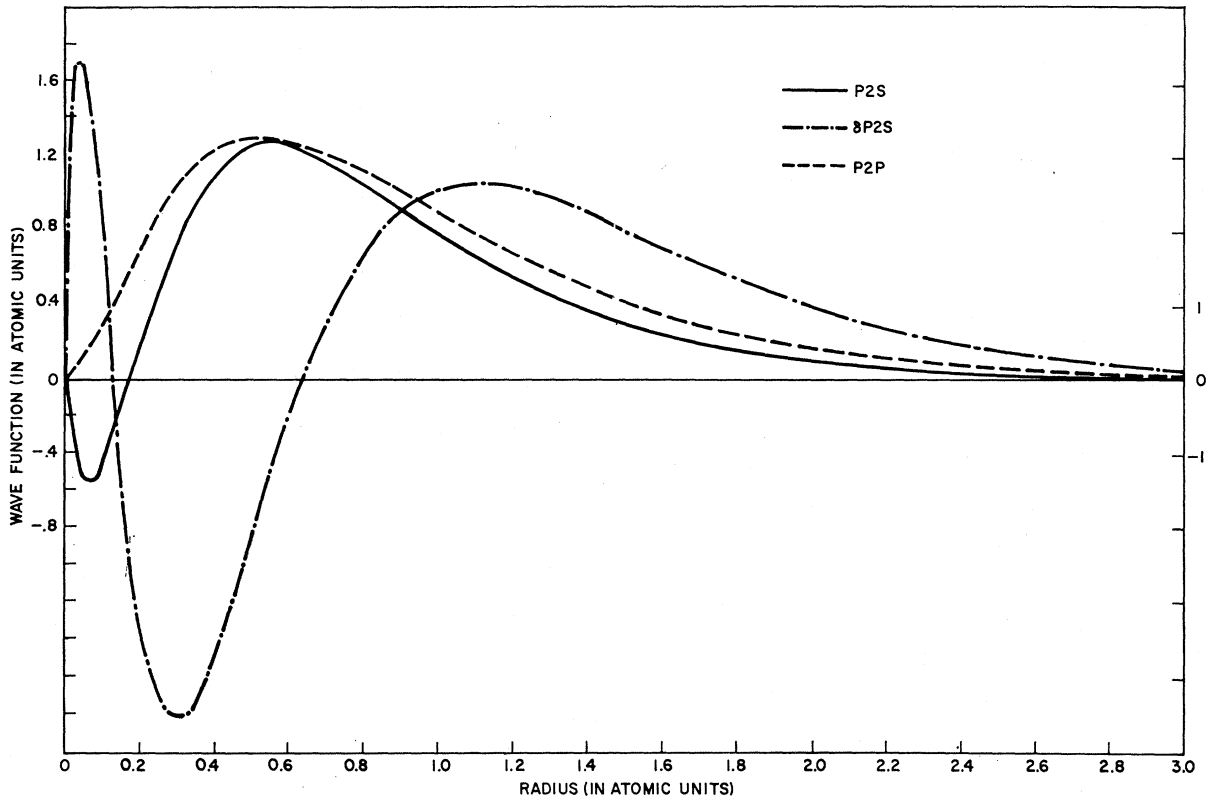

FIG. 4. Unperturbed P_{2s}, P_{2p} and moment perturbed δP_{2s} states for magnesium. (Referred to U_{2s}, U_{2p} and δU_{2s} in the text.)

term involving the perturbed $1s$ core was larger than the corresponding ratio for the $2s$ core. The same explanation for this effect as that advanced for the alkali atoms[27] and alkali metals would also apply here. The direct and cp contributions from various points on the Fermi surface in beryllium have already been published.[8] For the sake of completeness we shall merely quote the total spin densities from the two segments of the Fermi surface referred to as cigars and coronet.

In Table III, the segmentwise contributions from the cp, direct and total terms have been listed after multiplying by the weighting factors related to the surface areas of these segments. The various types of contributions to the spin density from the entire Fermi surface can thus be obtained from listed contributions from individual segments by vertical addition as indicated in the last row of the table. Particularly meaningful for the analysis of the relaxation time and the Korringa constant[23] in Sec. IV, are the total spin densities from the s, p, and d components of the conduction-electron wave functions, shown in the last row of the Table III.

For magnesium, it is interesting to examine the relative signs and magnitudes of contributions to S_{cp} from the exchange polarization of the $1s$ and $2s$ cores by the s, p, and d components of the conduction-electron wave function. For this purpose, these various contributions to S_{cp} are listed in Table V for one typical point on each of the segments of the Fermi surface. The following features may be noted for S_{cp} from Table V. Under the influence of the polarizing effect of the s component of Ψ_{cond}, both $1s$ and $2s$ cores lead to positive spin densities, the latter being usually a factor of 3 larger than the former. For the p component of Ψ_{cond}, the cp contributions from $1s$ and $2s$ cores have opposite signs, the latter being positive and more than an order of magnitude larger than the former. The net S_{cp} associated with the p part of Ψ_{cond} is, therefore, *positive* as in the case of aluminum,[24] but opposite in sign to that assumed for metals with d bands.

While these observations regarding the signs and the relative magnitudes of various cp terms are obtained from actual numerical calculations, they could have been anticipated from the radial characters of the mp and unperturbed atomic functions in Figs. 3 and 4. The latter functions are also representative of the behavior of conduction-electron OPW functions in the core regions. Thus, an examination of Eq. (24) and the plots in Fig. 4 reveals that the exchange-polarization integral for the $2s$ state derives its contribution from a positive region in the outer parts of the ion core and negative region in the inner part. The former region can be seen

[27] L. Tterlikkis, S. D. Mahanti, and T. P. Das, Phys. Rev. **176**, 10 (1968).

TABLE V. cp contribution from s, p, and d parts of Ψ_{cond} to spin density in magnesium from $1s$ and $2s$ cores for some typical representative points.

Coordinate	Segment	cp contributions from $1s$ core			cp contributions from $2s$ core		
		s	p	d	s	p	d
(0, 0, 0.058)	Lens	0.3920×10^{-1}	-0.4110×10^{-3}	0.4693×10^{-3}	0.1201	0.1647×10^{-1}	-0.4314×10^{-3}
(0.6221, 0, 0)	Cigar	0.1532×10^{-1}	-0.2108×10^{-3}	0.2020×10^{-3}	0.4840×10^{-1}	0.6258×10^{-1}	-0.2336×10^{-3}
(0.5213, 0.301, 0.2921)	Butterfly	0.4560×10^{-1}	-0.4429×10^{-3}	0.5298×10^{-3}	0.1403	0.1250×10^{-1}	-0.5033×10^{-3}
(0.3914, 0.226, 0)	Monster	0.3756×10^{-2}	-0.1839×10^{-2}	0.1698×10^{-3}	0.1174×10^{-1}	0.6038×10^{-1}	-0.1961×10^{-3}

to occupy more phase space, and thus to determine the over-all sign of the cp contribution. The $1s$ cp contribution, because of the small values of r over which the $1s$ wave function is confined, derives major contributions from the negative part of $\delta U_{1s}(r)$ and hence has a negative sign. Similar examination of the cp effect for the s part of Ψ_{cond} can help explain the difference in nature of the observed ratios of the $1s$ and $2s$ cp contributions from the s and p components of Ψ_{cond}. Our calculated contributions to the spin density from the direct and cp terms are listed in Table II for all the 15 points on the Fermi surface that we have analyzed. Also listed for reference are the $\mathbf{k}$-dependent density-of-states functions $1/|\nabla_k E|$ which are needed for the averaging procedure in Eq. (9). In Table IV, we have listed the average direct and cp contributions from each segment of the Fermi surface. Because of their importance in the interpretation of T_1T and the Korringa constant, the contributions to S_{cp} from the s, p, and d components are again presented separately. Unlike Table III for beryllium, the spin densities listed in Table IV for the various segments of the Fermi surface have not been multiplied by the weighting factors associated with the relative areas. Instead, we have listed the two sets of areas of the segments described in Sec. II, which may be utilized to obtain the net Fermi surface average.

Several comments may be made about the results for magnesium in Tables II and IV. The variation in the direct and the cp contributions over various points considered for the lens, cigar, and butterflies is not very marked. The monster which spans a number of different parts of the Brillouin zone shows more variations in the spin density. We have, therefore, utilized more points in the averaging procedure for monster than for other cases. The contributions from the four segments of the Fermi surface indicate that the lens and butterflies have primarily s character. The monster and cigars, on the other hand, have more p and d characters and thus make relatively small contributions to the direct spin density. The d contribution is seen to be orders of magnitude less than the p and s contributions and, therefore, the neglect of higher angular components f, g, ... is justified. The over-all cp contribution frmo the s component of the wave function is seen to be comparable to the cp result from the p component. However, for the Korringa constant the ratio of $S_{cp}{}^p$ to the sum of S_d and $S_{cp}{}^s$ is important. This ratio, obtained by combining contributions from the various segments, is seen from Table VI to be $\frac{1}{6}$ and positive.

IV. SPIN SUSCEPTIBILITY AND EXCHANGE-ENHANCEMENT EFFECTS

Both K_s and T_1 are expected to be influenced by the effect of electron-electron interaction on the response of the electrons to a magnetic field. This effect is usually referred to as exchange enhancement and for K_s it is the exchange enhancement of the Pauli spin susceptibility $\chi_p{}^*$ that has to be considered. The basic difference between the exchange-enhancement processes for χ_p and T_1 can be understood as follows: χ_p is the response of the conduction electrons to a uniform static magnetic field. On the other hand, for the case of relaxation time T_1, the electrons can be thought of responding to the fluctuating inhomogeneous magnetic field produced by the nucleus. The relevant response function in this case is not χ_p but $\chi(\mathbf{q},\omega)$ where χ_p is the static and uniform limit of $\chi(\mathbf{q},\omega)$, i.e.,

$$\chi_p=\chi(0,0). \tag{27}$$

We shall consider the exchange enhancements of $\chi(0,0)$ and $\chi(\mathbf{q},\omega)$ separately.

A proper treatment of the exchange enhancement of χ_p would require the solution of the problem of Bloch electrons in a magnetic field. There are two difficulties connected with this problem. First, the ordinary metallic densities do not correspond to the extreme limits of high and low densities, where one can solve the many-body problem for a uniform electron gas with fair accuracy. Secondly, there is the problem of the departure of an actual system from a uniform electron gas, a consequence of the lattice potential which leads to the band structure. We shall utilize the exchange-enhancement results of Silverstein,[9] and use an effective-mass approximation to incorporate the effects of band structure.

Silverstein's expression[9] for the exchange enhanced susceptibility $\chi_p{}^*$ is

$$\chi_p{}^*=\frac{\chi_p}{1+(m/m^*-1)\chi_p/\chi_f}. \tag{28}$$

In Eq. (28), χ_f is the free-electron susceptibility appropiate to the density of conduction electrons in the

TABLE VI. Direct and cp contribution to Knight shift in beryllium and magnesium.

Metal	K_s^d (in %)	K_s^{cp} (in %) s	p	d	K_s^{tot} (in %)	K_s^{expt} (in %)
Beryllium	0.9444×10^{-3}	0.1786×10^{-3}	-0.3856×10^{-3}	-0.0200×10^{-3}	$+0.71\times10^{-3}$	-0.0025
Magnesium	0.3818×10^{-1}	0.9558×10^{-2}	$+0.8020\times10^{-2}$	-0.3804×10^{-3}	$+0.5538\times10^{-1}$	$+0.112$

metal. χ_p is the exchange enhanced susceptibility in the free-electron approximation. The factor (m/m^*-1) in the denominator takes account of band effects. It should be noted that if one puts $\chi_p=\chi_f$, then Eq. (28) gives

$$\chi_p^*=\chi_f(m^*/m)=\chi_{\text{band}}, \tag{29}$$

which is the unenhanced band susceptibility. Since

$$m^*/m=g(E_F)\,|_{\text{metal}}/g(E_F)\,|_{\text{free}}, \tag{30}$$

where

$$g(E_F)=(dn/dE)_{E=E_F}, \tag{31}$$

the incorporation of the factor (m/m^*-1) in Eq. (28) introduces band effects on the unenhanced susceptibility, and also indirectly includes the effect of the lattice potential on the exchange enhancement. For purposes of understanding the origin of exchange enhancement of the relaxation rate, to be discussed later in the section, it is helfpul to define two parameters α and α^* as

$$\alpha=1-\chi_f/\chi_p, \tag{32}$$

$$\alpha^*=(m^*/m)\alpha. \tag{33}$$

Since Silverstein's[9] expression uses the effective-mass approximation, it is expected to be most valid for metals whose band structures are nearly free-electron–like. Thus, there is evidence that Silverstein's result is reasonably satisfactory for alkali metals. For magnesium, even though we have (essentially) two bands at the Fermi surface, the fair agreement between the Harrison construction and the actual band structure over most part of the Fermi surface leads one to expect that Silverstein's expression may be satisfactory in this case. No theoretical results are available for magnesium. We have, therefore, used available low-temperature specific-heat data and the relation

$$\gamma=\tfrac{1}{3}\pi^2k_B^2g(E_F)(1+\lambda) \tag{34}$$

to obtain $g(E_F)$. In Eq. (34), $\gamma=C_P/T$, where C_P is the specific heat, and λ is the enhancement factor of the specific heat due to electron-phonon interaction. Two values are available for γ. The most recent one, obtained by Martin,[28] is 292.7 ± 2.5 cal deg^{-2} g-at.$^{-1}$, about 11% lower than the somewhat earlier results of Esterman *et al.*,[29] and we have chosen Martin's value for calculation of $g(E_F)$. We have used $\lambda=0.3$ which was obtained by Kimball *et al.*[18] from comparison of cyclotron-mass and band-mass data at some representative points on the Fermi surface. This value of λ for magnesium is consistent with theoretical estimates by McMillan[30] for the adjacent metals, sodium and aluminum. In this manner we have obtained

$$g(E_F)=53.7959\times10^{32}, \tag{35}$$

which corresponds to

$$(m^*/m)=0.946. \tag{36}$$

The ratio m^*/m found in this manner is nearly equal to 1. This gives us added confidence in the applicability of Silverstein's expression. From the curves in Silverstein's paper for χ_f and χ_p versus r_s, for magnesium ($r_s=2.64$)

$$\chi_p=1.325\times10^{-6} \text{ cgs volume units} \tag{37}$$

and

$$\chi_f=0.9788\times10^{-6} \text{ cgs volume units} \tag{38}$$

leading to a free-electron enhancement parameter

$$\alpha=0.2613. \tag{39}$$

On substituting these values of χ_p and χ_f in Eq. (28) together with the value of (m^*/m) from Eq. (36), we get

$$\chi_p^*=1.2299\times10^{-6} \text{ cgs volume units} \tag{40}$$

and

$$\alpha^*=0.2472. \tag{41}$$

The corresponding value for χ_{band} is

$$\chi_{\text{band}}=0.9259\times10^{-6} \text{ cgs volume units.} \tag{42}$$

It is to be noted that from these results we obtain

$$\alpha^*/\alpha=m^*/m=0.946, \tag{43}$$

indicating that there is only about a 6% decrease in the parameter α due to the interplay of band and exchange-enhancement effects. Also we obtain

$$\chi_p^*/\chi_{\text{band}}=\eta_s=1.3283. \tag{44}$$

When a more detailed theory of exchange enhancement for Bloch electrons is available, it would be interesting

[28] D. L. Martin, Proc. Roy. Soc. (London) **78**, 1482 (1961).
[29] I. Eastermann, S. A. Driedberg, and J. E. Goldman, Phys. Rev. **87**, 582 (1952).
[30] W. L. McMillan, Phys. Rev. **167**, 331 (1968).

to see how closely its predictions agree with the numbers in Eqs. (43) and (44).

No experimental value is available for the spin susceptibility to compare with χ_p^*. Two recent experimental values[31,32] (in good agreement with each other) are available for the total susceptibility χ_{total} given by

$$\chi_{\text{total}}=\chi_{\text{ion}}+\chi_{\text{orb-dia}}+\chi_p^*, \tag{45}$$

where χ_{ion} and $\chi_{\text{orb-dia}}$ are, respectively, the ion-core and orbital contributions. The ionic contribution χ_{ion} is given by

$$\chi_{\text{ion}}=-(e^2a_0^2N/6mc^2)\times(2\langle r^2\rangle_{1s}+2\langle r^2\rangle_{2s}+6\langle r^2\rangle_{2p})\ \text{emu/mole}, \tag{46}$$

where $\langle r^2\rangle_i$ represents the expectation value of r^2 for core electrons in a state i. On substituting for the expectation values taken over the $1s$, $2s$, and $2p$ atomic core functions of Clementi,[33] we get

$$\chi_{\text{ion}}=-0.2709\times10^{-6}\ \text{cgs volume units}. \tag{47}$$

The orbital part of the susceptibility is difficult to evaluate exactly. If one uses the simple result

$$\chi_{\text{Landau}}=-\tfrac{1}{3}\chi_f \tag{48}$$

for free electrons, one obtains from Eq. (45), using Eqs. (47) and (48) and Burr and Orbach's[21] recent value of

$$\chi_{\text{total}}=0.9658\times10^{-6}\ \text{cgs volume units}, \tag{49}$$

a predicted value for the spin susceptibility

$$\chi_p^*=1.5867\times10^{-6}\ \text{cgs volume units}. \tag{50}$$

This value is about 30% larger than the theoretical value in Eq. (40). One possible reason for this discrepancy is the simple approximation of using χ_{Landau} for $\chi_{\text{orb-dia}}$.[34] Actually, detail treatments of $\chi_{\text{orb-dia}}$ indicate that there are a number of other terms which can contribute comparable amounts. Part of the disagreement could, however, be due to a possible inaccuracy in our result for χ_p^* given in Eq. (40). An experimental measurement of the spin susceptibility would be very helpful in this connection.

The exchange-enhancement situation in beryllium is more complex than in magnesium. In beryllium, the effective mass[13] departs strongly from the free-electron value and the Harrison construction[21] does not reproduce the actual Fermi surface. These strong departures from free-electron character suggest that Silverstein's expression[9] would not be applicable for beryllium. In fact, the experimental[35] value of the spin susceptibility from ESR experiments is

$$\chi_{\text{expt}}^*=2\times10^{-7}\ \text{cgs volume units} \tag{51}$$

as compared to the band value

$$\chi_{\text{band}}=6.36\times10^{-7}\ \text{cgs volume units} \tag{52}$$

obtained by using the band-structure density of states. This value is in reasonable agreement with 5.2×10^{-7} cgs volume units, which is obtained from the specific-heat measurements of Hill and Smith,[36] after correcting for the phonon effects. There are two other measurements of specific heat by Gmelin[37] and Falge[38] and using their values and appropriate phonon corrections, one obtains for χ_{band}, 4.2×10^{-7} and 4.8×10^{-7} cgs volume units, respectively. A comparison of experimental χ_p and different available values of χ_{band} indicates that there is a strong deenhancement of the susceptibility due to exchange, rather than the enhancement predicted from the physical consideration for an electron gas. Normally, one expects the exchange interaction between the electrons to be attractive and hence to lead to a stronger alignment of the electrons in a magnetic field than would be the case for noninteracting electrons. The deenhancement effect in beryllium suggests that the crystalline potential leads to an apparent antiferromagnetic exchange interaction between the electrons. Evidently, a thorough treatment of interacting Bloch electrons in a magnetic field is necessary for a proper understanding of the situation in beryllium. In our calculation of the Knight shift, we have avoided this question and made use of the experimental result[35] for the spin susceptibility.

For the exchange-enhancement effects associated with the relaxation rate $(T_1)^{-1}$ as mentioned earlier, we require a knowledge of $\chi(\mathbf{q},\omega)$. Since the important frequency range for the relaxation process is in the neighborhood of the nuclear Larmor frequency ω_L, which is slow compared with the motion of the interacting electrons, we can effectively use $\chi(\mathbf{q},0)$. Moriya has carried out an evaluation[39] of $\chi(\mathbf{q},0)$ using a δ-function approximation to the screened exchange potential between the electrons. This is a reasonable approximation to the short-range screened exchange interaction between electrons in a metal. Narath and Weaver[40] and Mahanti and Das[2] have already applied Moriya's[39] theory to alkali metals where the exchange enhancement is found to substantially improve agreement between theory and experiment. The expression derived by Moriya, including exchange-enhancement effects, is

$$(T_1T)_{\text{Moriya}}^{-1}=(T_1T)_{\text{cont}}^{-1}(\eta_M), \tag{53}$$

where

$$\eta_M=\langle[1-\alpha^*F(q)]^{-2}\rangle_{\text{av}}. \tag{54}$$

[31] C. R. Burr and R. Orbach, Phys. Rev. Letters **19**, 1133 (1967).
[32] B. I. Vyerkin and I. V. Svyechokarov, Ukr. Fiz. Zh. **7**, 322 (1962).
[33] E. Clementi, IBM J. Res. Develop. **9**, 2 (1965).
[34] J. E. Hebborn and M. J. Stephen, Proc. Roy. Soc. (London) **80**, 991 (1962).
[35] G. Feher and A. F. Kip, Phys. Rev. **98**, 337 (1955).
[36] R. W. Hill and P. L. Smith, Phil. Mag. **44**, 636 (1953).
[37] E. Gmelin, Compt. Rend. **259**, 3459 (1964).
[38] R. L. Falge, Jr., Phys. Letters **24**, 579 (1967).
[39] T. Moriya, J. Phys. Soc. Japan **18**, 516 (1963).
[40] A. Narath and H. T. Weaver, Phys. Rev. **175**, 373 (1968).

TABLE VII. Results for the relaxation rate in beryllium and magnesium.

Metal	$(1/T_1T)_d$	$(1/T_1T)_{d+\mathrm{cp},s}$	$(1/T_1T)_{\mathrm{cp},p}$	$(1/T_1T)_{\mathrm{tot}}$	$(T_1T)_{\mathrm{tot}}$	$(T_1T)_{\mathrm{tot}}^{\mathrm{Moriya}}$	$(T_1T)_{\mathrm{expt}}$
Beryllium	0.6781×10^{-4}	0.9588×10^{-4}	0.1130×10^{-4}	0.9965×10^{-4}	1.0035×10^{4}	0.8726×10^{4}	$(1.66+0.2)\times10^{4}$
Magnesium	1.1765×10^{-3}	1.8392×10^{-3}	0.0519×10^{-3}	1.8565×10^{-3}	0.5386×10^{3}	0.3458×10^{3}	...

The parameter α^* in Eq. (54) is the same as in (41). The function $F(q)$ is the linear dielectric function which, for a spherical Fermi surface, is given by

$$F(q)=\frac{1}{2}\left(1+\frac{4k_F{}^2-q^2}{4k_Fq}\ln\left|\frac{2k_F+q}{2k_F-q}\right|\right). \tag{55}$$

The average in Eq. (54) is carried out over all values of q which are consistent with the energy conservation relation

$$E(\mathbf{k}_F+\mathbf{q})-E(\mathbf{k}_F)=\pm\hbar\omega_L\approx0. \tag{56}$$

For a spherical Fermi surface, the range of q in keeping with the condition is 0 to $2k_F$. The enhancement factor for $(T_1T)^{-1}$ is small compared to that for K_s, because $F(q)$ decreases as q increases. This result has an important bearing on the Korringa constant[23] and would lead to a departure from the value, $(\hbar/4\pi k_B)(\gamma_e/\gamma_N)^2$ of the latter for noninteracting electrons.

For magnesium, we have used the value of α^* in Eq. (48) leading to

$$\eta_M=1.5573.$$

For beryllium, the calculation of η_M presents some problems due to the uncertainties discussed earlier for the exchange enhancement of χ_p. In Sec. V we have presented results for beryllium both for $\alpha^*=0$ which corresponds to no enhancement and $\alpha^*=0.0846$ from Eq. (33) using pertinent values of m^*/m and α for beryllium.

V. RESULTS AND DISCUSSIONS

The Knight shift and the relaxation time including the effects of cp can be obtained from a knowledge of the spin densities determined in Secs. II and III. The corresponding expressions are

$$K_s=K_s{}^d+K_s{}^{\mathrm{cp}}=(8\pi/3)\chi_p{}^*\Omega_0S, \tag{57}$$

where

$$S=S_d+S_{\mathrm{cp}}{}^s+S_{\mathrm{cp}}{}^p+S_{\mathrm{cp}}{}^d$$

and

$$(T_1T)^{-1}=AG,$$

with

$$G=(S_d+S_{\mathrm{cp}}{}^s)^2+\tfrac{1}{3}(S_{\mathrm{cp}}{}^p)^2+\tfrac{1}{5}(S_{\mathrm{cp}}{}^d)^2. \tag{58}$$

The quantity A has already been defined in Eq. (15). In Eq. (57), either the experimental susceptibility, if available, or the theoretical susceptibility including exchange-enhancement effects[9] have to be utilized. For beryllium the experimental susceptibility[35] $\chi_p{}^*$ is available while for magnesium we have utilized the value obtained from the low-temperature specific-heat (γT) data after applying corrections for the electron-phonon enhancement to γ and the exchange-enhancement effects to the susceptibility. These values have already been discussed in Sec. IV. For the relaxation time, one again has to apply a correction for exchange-enhancement effects. The nature of this enhancement has been discussed by Moriya[39] and others and a value for the corresponding enhancement factor has been obtained for magnesium in Sec. IV. For beryllium the situation is somewhat uncertain in view of the apparent de-enhancement effect derived from the experimental susceptibility while the available theoretical treatments predict an enhancement. The corresponding treatment of exchange effects[39] on $(T_1T)^{-1}$ also leads to an enhancement factor of 1.15 derived in Sec. IV. These uncertainties have to be borne in mind while comparing theoretical and experimental values of K_s and T_1. The dissimilarity in the influence of cp effect on K_s and T_1 apparent from Eqs. (57) and (58) is expected to have a significant bearing on the Korringa constant[23] when the non-s cp is significant.

In Tables VI and VII we have listed the various contributions to K_s and $(T_1T)^{-1}$ in beryllium and magnesium using Eqs. (57) and (58), and the spin densities obtained in Secs. II and III. We shall consider the results in beryllium first. The p-cp makes a substantial negative contribution to the Knight shift which is larger than the s-cp in magnitude and about one-third that of the direct contribution. The reason for this pronounced p-cp is that both the coronet and cigars have sizable areas over which the p character is preponderant.[8] However, the negative p contribution from $K_s{}^{\mathrm{cp},p}$ is not enough to counterbalance the positive $K_s{}^d$ to lead to the negative sign that is observed experimentally.[41,42]

One, therefore, has to invoke other contributing mechanisms, such as the orbital Landau-type[34] effect to explain the experimental negative sign. The alternative explanation that we might have made an underestimation of $K_s{}^{\mathrm{cp},p}$ does not seem likely, in view of our careful scanning of the Fermi surface and the accuracy with which the features of the Fermi surface can be explained by OPW band calculation. Additionally, such an explanation will be shown to widen the gap between theory and experiment for T_1.

[41] W. T. Anderson, Jr., M. Ruhlig, and R. R. Hewitt, Phys. Rev. **161**, 293 (1967).

[42] D. E. Barnaal, R. G. Barnes, B. R. McCart, L. W. Mohn, and D. R. Torgeson, Phys. Rev. **157**, 510 (1967).

The results for the relaxation time, listed in Table VII complement the results for Knight shift in providing an estimate of the importance of the various mechanisms that contribute to the hyperfine effects in this metal. The p-cp contribution to $(T_1T)^{-1}$ is found to be less effective than in the case of K_s as expected from Eqs. (57) and (58). An increase in the magnitude of $S_{cp}{}^p$ would increase the p contribution to $(T_1T)^{-1}$ and thus widen the disagreement between experiment and theory. The theoretical value of $(T_1T)^{-1}$ is in reasonable agreement, but a factor of $\frac{3}{2}$ higher than the experiment. A possible reason for this discrepancy is that our estimate of S_d and $S_{cp}{}^s$ might be too large. As emphasized before in discussing K_s, we do not believe that this is the case. Orbital and dipolar contributions to the relaxation time[43] are expected to be small because they involve $\langle 1/r^3 \rangle$ which is very small for a light metal like beryllium. In addition, their inclusion would increase $(T_1T)^{-1}$ in a direction opposite to the experiment. We believe that the main reason for the remaining discrepancy with experiment is the presence of an exchange-deenhancement effect similar to that observed for χ_p. Since the square of a conduction-electron matrix element is involved in $(T_1T)^{-1}$, the use of the same deenhancement factor as χ_p for the spin matrix element would lead to much too small a value for $(T_1T)^{-1}$ as compared to the experiment. It thus appears that a much feebler deenhancement effect seems to be occurring for $(T_1T)^{-1}$ as compared to χ_p.

A comparison between the theoretical and experimental Korringa constant $K_s{}^2T_1T$ is not very meaningful at the present time for beryllium for two reasons. First, there are the uncertainties connected with the exchange-deenchancement effects for both K_s and $(T_1T)^{-1}$. Secondly the exact influence of orbital contributions[34] to K_s is not known, leading to the discrepancy between the sign of the experimental and theoretical values, the latter obtained from purely spin effects. However, to demonstrate the influence of cp on the Korringa constant[23] and in particular the difference in behavior of beryllium and magnesium in this respect, it is helpful to compare the values of $K_s{}^2T_1T$ with and without including cp effects. The values of these quantities are 0.5115×10^{-5} and 1.33×10^{-5}, respectively; the former value being smaller because we have a negative p-cp effect. The corresponding situation in magnesium will be seen to be opposite in nature.

The Knight shift results on magnesium in Table VI show significant qualitative differences from those on beryllium. One significant difference is the positive cp contribution from the p character of the conduction-electron wave function in contrast to the negative contribution for beryllium. This difference in behavior has a profound effect on the total Knight shift. In particular, the s and p contributions from the monster which account for the major area of the Fermi surface now reinforce each other in contrast to the cancellation of these contributions from the coronet in beryllium (which is the counter part of monster in magnesium). In beryllium, the other important segment of the Fermi surface was composed of cigars which had larger amounts of s character than the coronet, but still smaller compared to the p character so that there was again a substantial cancelling effect. In magnesium, on the other hand, the remainder of the Fermi surface is composed of butterflies, lens, and cigars.[14,18] The lens and the butterflies are seen to have much stronger s character than the cigar in beryllium. The cigars in magnesium have smaller relative area than in beryllium, but the positive sign of the p-cp helps in making their contributions quite important. Thus we see that a combination of these two features—the larger amount of s character, and the positive cp due to p character—provide a qualitative explanation of the positive and substantial Knight shift in magnesium, in contrast to the situation in beryllium.

We next turn our attention to a comparison between our theoretical result of K_s and the experiment and the possible importance of other mechanisms that could contribute to the Knight shift. In this connection it is interesting to note that the relative areas of various segments of the Fermi surface have a significant role in determining the values of the direct and cp contribution to the Knight shift. This is because the lens and the butterflies have substantial s character and their relative contributions are determined by their areas as compared to the monster which seems to be predominantly non-s in character. Thus, if one uses the relative areas obtained from the Harrison's one OPW construction,[21] ironically the Knight shift (0.0784%) is in better agreement with experiment than our value in Table VI which was obtained by using areas determined from the magnetoacoustic attenuation measurements of Ketterson and Stark.[19] Since the dimensions predicted by OPW calculations using Falicov's[14] potential are in substantial agreement with Ketterson and Stark's experimental dimension for several parts of the Fermi surface, this acts as a check on both the correctness of the wave functions that we have used for our calculation and the relative areas used in our averaging procedure. The value for K_s in Table VI is, therefore, more acceptable than the apparently better value calculated by using the surface areas from Harrison's construction. As regards the calculation of the cp contribution, the mp procedure[7] adopted here has been tested by applications to atoms and other metals. In other metals, it gives corrections in the right direction and about the right magnitude to improve agreement with the experiment. For atoms, it has been found to give results in good agreement with cp contributions calculated by diagrammatic perturbation theory techniques[44] and, in

[43] A. Abragam, *The Principles of Nuclear Magnetism* (Oxford University Press, Oxford, 1961).

[44] N. C. Dutta, C. Matsubara, R. T. Pu, and T. P. Das, Phys. Rev. Letters **21**, 1139 (1968).

several instances, with the results of the unrestricted Hartree-Fock method.[45] A conservative estimate is that our cp result is accurate to within 10% which is a much smaller fraction of the total K_s. One must, therefore, look for other causes for an explanation of the difference between the theoretical value, 0.0564%, and the experimental value, 0.112%.

In looking for sources to explain the difference between the theory and experiment,[46,47] there are two categories to consider. In the first, are the possible inaccuracies in the quantities and procedures we have already used for evaluating the direct and cp contributions and in the second are the additional mechanisms contributing to K_s. As regards the first category, we have already pointed out that there is not much likelihood of any significant inaccuracy in our spin-density calculation. The major uncertainty is in the spin susceptibility χ_p^*. Since a calculated density of states is not available, we have had to use the specific-heat data[28] with an approximate correction[18] for the electron-phonon enhancements. But even more serious is the question of exchange enhancements to be applied to χ_p. The effective mass in magnesium is close to unity. The Fermi surface exhibits fewer gaps and a closer resemblance to free-electron–type behavior than in beryllium. There is, therefore, reason to believe that the exchange-enhancement approach of Silverstein is more justifiable for magnesium than for beryllium. However, an experimental measurement of χ_p^* would be helpful to remove this uncertainty. Until such a measurement is available, it is difficult to assess the role of other mechanisms for K_s and our subsequent comments are to be considered somewhat tentative. It is interesting, however, that $\chi_p^*=1.5867\times10^{-6}$ cgs volume units calculated from the total susceptibility is somewhat larger than the value $\chi_p^*=1.2299\times10^{-6}$ cgs volume units we have been using based on the specific-heat data. While the use of total χ to obtain χ_p^* has uncertainties due to the orbital contributions, the difference between the two values of χ_p^* is in the right direction to improve the Knight shift value.

Among additional mechanisms that could contribute to the Knight shift, one possibility is a mechanism analogous to the cp effect considered already. The conduction electrons below the Fermi surface can be exchange polarized[48] by the surplus electrons of one spin at the Fermi surface in the presence of the magnetic field. This mechanism is similar to the polarization of the s-band electrons by the magnetic d electrons in ferromagnets. Unfortunately, it is difficult to apply the mp procedure to this problem because the electrons that are being perturbed are not localized as were the core electrons and one cannot obtain simple radial differential equations to describe the perturbation by the nuclear moment. One has, therefore, to adopt other methods. This effect may be seen easily to vanish for free electrons since the exchange potential cannot, by itself, perturb the plane waves. The Bloch electrons, however, can be perturbed by the exchange-polarization potential, and the spin density at the nucleus due to this mechanism will be proportional to the second-order energy

$$\delta^2E=\frac{\chi_{pH}}{\mu_B}\sum_{i,j,n}\frac{\langle k_{Fi}(1)k_j(2)|r_{12}^{-1}|k_j^n(1)k_{Fi}(2)\rangle\langle k_j^n(1)|H_N(1)|k_j(1)\rangle}{E_j^n-E_j}, \tag{59}$$

where k_{Fi} represents a particular state at the Fermi surface, k_j an occupied conduction-electron state *below* the Fermi surface, and k_j^n an unoccupied state with the same reduced vector k_j, but belonging to an empty band above the Fermi surface. The energy difference $(E_j^n-E_j)$ represents the vertical interband excitation energy for the state k_j, the summations i and j refer to the states on the Fermi surface and below it, respectively, while n runs over all the excited bands. This conduction-conduction exchange-polarization mechanism[48] appears to be quite sensitive to the band gaps $(E_j^n-E_j)$ and could derive significant contributions from regions where the gaps between occupied and unoccupied bands are small. From the calculated band structure of magnesium, there are only a few regions with small band gaps. It is difficult to estimate the exact magnitude of the contribution from this mechanism without actual calculation, since the convergence in n is determined both by the numerator and the denominator of Eq. (59). One thus requires a detailed knowledge of the energies and wave functions of the excited bands for all of $\mathbf{k}$ space. We could, however, speculate qualitatively on the importance of this mechanism by analogy with beryllium. Regions of small band gaps at the Fermi surface are more pronounced in beryllium and if this conduction-conduction exchange mechanism were important, it would be expected to make more significant relative contribution compared to other mechanisms in beryllium. If this were true, then the theoretical K_s would be altered markedly from the near-zero value that has been obtained, bringing it into qualitative disagreement with experiment. It seems to us that the conduction-conduction exchange-polariza-

[45] M. H. Cohen, D. A. Goodings, and V. Heine, Proc. Phys. Soc. (London) **73**, 811 (1959).
[46] T. J. Rowland, in *Progress in Material Science*, edited by Bruce Chalmers (Pergamon Press, Inc., New York, 1961), Vol. IX, p. 14.
[47] P. D. Dougan, S. N. Sharma, and D. L. Williams, Can. J. Phys. (to be published).
[48] S. H. Vosko and R. A. Moore, Bull. Am. Phys. Soc. **12**, 314 (1967).

tion mechanism is unlikely to be responsible for any major part of the difference between experiment[46,47] and theory in magnesium.

Another possible source of contribution to the Knight shift is through the nuclear-electron orbit interaction.[34] A quantitative evaluation of this effect would require the calculation of the complicated interband and intraband terms in the generalized expression derived by Hebborn and Stephen.[34] However, for qualitative discussion, the orbital effects could be divided into two parts, a Landau-type effect characteristic of the continuous nature of the energy levels in the bands and a Van Vleck–Ramsey type interband contribution analogous to the chemical shift effect in molecules. The Landau-type effect is pronounced only if the effective mass of the conduction electron is small compared to the free-electron mass. Since m^*/m in magnesium is close to unity, it is safe to conclude that the Landau-type effect is not significant in this metal.

The Van Vleck–Ramsey type orbital contribution Eq. (59), the exchange matrix element being replaced by a matrix element involving the magnetic field. Again, it is difficult to decide on the actual importance of this mechanism without explicit calculation. Since there seems to be substantial non-s character on the monster which is necessary for the orbital contribution to be finite, this orbital effect is likely to be more important than the conduction-conduction polarization mechanism.

Finally, there could be some contribution to the spin density from the correlation[2] between the core electrons and the spin polarized conduction electrons at the Fermi surface. This is rather a difficult effect to calculate because it requires an analysis of the many-body effect involving both the core and conduction electrons in the presence of a magnetic field. However, an estimate of the importance of this mechanism can be made by comparison with core-valence correlation contributions to the hyperfine interaction in sodium atom.[27] In sodium atom, a comparison of the theoretical hyperfine constant including direct and cp effects with the experiment indicates that the correlation effect is about 15% of the direct plus cp effect. Since the conduction electrons of magnesium on the Fermi surface involve both p and d characters as well as s, the percentage importance of this correlation effect can be somewhat different. Nevertheless, an estimated 10–15% contribution to the Knight shift from core-conduction correlation effects seems reasonable.

In summary, it is our feeling that while a combination of orbital[34] and core-conduction correlation[2] effects could explain a reasonable part of the difference between the theoretical K_s in Table VI and the experiment, the main source of correction is quite likely to come out of a change in the Pauli susceptibility χ_p.

Unfortunately, no measurement of the relaxation time T_1 is currently available for comparison with our theoretical value. However, Dougan, Sharma, and Williams[47] have mentioned that they had distortion due to saturation at 1.2°K indicating a long relaxation time T_1. Our calculated value of T_1T would lead to $T_1=288.2$ sec at 1.2°K and 82.3 sec at 4.2°K, the temperature at which Dougan *et al.*[47] carried out their measurement.

The following observations may be made regarding the nature of the theoretical T_1. The positive cp contribution to the spin density from the p component of the conduction-electron wave function does not affect $(T_1T)^{-1}$ as markedly as it does K_s. This is because of the dependence of $(T_1T)^{-1}$ on the square of $S_{cp}{}^p$ instead of linear as in the case of K_s. This, of course, will have important consequences for the Korringa constant, to be discussed later in this section. While the evidence is not clear cut, the Knight shift K_s appears to have been underestimated as a result of a corresponding underestimation in the theoretical $\chi_p{}^*$. For the relaxation time it is the $\mathbf{q}$-dependent spin susceptibility $\chi(\mathbf{q})$ in the range $\mathbf{q}=0$ to $\mathbf{q}=2\mathbf{k}_f$ which is important, and one expects a similar underestimation in $\chi(\mathbf{q})$ as in χ_p. In addition to this uncertainty, the other contributing factors such as the conduction-conduction polarization[48] and the orbital relaxation process and core-conduction correlation[2] which could have appreciable effect on the Knight shift are also expected to influence T_1. However, the s and non-s components of the conduction-electron wave function are expected to influence $(T_1T)^{-1}$ in the same manner as in the case of cp mechanism in Eq. (42). Thus the influence of these additional mechanisms are expected to be less important for T_1 than for K_s, particularly the orbital effect[49] which has no contribution from the s component of the conduction-electron wave function. Considering all these factors and including the uncertainty in $\chi_p(\mathbf{q})$, we expect that our theoretical T_1 could be reduced by as much as a factor of 3. An experimental determination of T_1 will, therefore, be extremely useful in throwing light on the relative importance of these various factors that could contribute to it.

It is interesting to consider the Korringa constant[23] $K_s{}^2T_1T$ since it allows one to nearly cancel out the uncertainties associated with the spin density. Since no experimental measurement of T_1 is available we have no information about the correctness of the calculated $(K_s{}^2T_1T)_{\text{theor}}=1.06\times10^{-4}$, particularly its ratio with respect to $(K_s{}^2T_1T)_{\text{free}}=0.7013\times10^{-4}$. The departure of this ratio from unity is a product of the ratio 1.5110 between $\eta_s{}^2$ and η_M and the factor (S^2/G) arising from the spin-density components. The latter factor is found to be larger than unity because of the positive sign of $S_{cp}{}^p$. A negative sign of this latter quantity would have led to a value of (S^2/G) smaller than unity and pushed the Korringa constant towards a value smaller than the ideal case. A measurement of $K_s{}^2T_1T$ would, therefore, throw some light on this question of the sign of $S_{cp}{}^p$. The conduction-conduction polarization, the orbital

H. Mitchell, J. Chem. Phys. **26**, 1714 (1957).

and core-conduction correlation mechanisms would also have a similar type of effect on $K_s^2T_1T$ as the cp although the exact extent of their influence is not currently available.

VI. CONCLUSION

The wave functions of the conduction electrons on the Fermi surface of beryllium and magnesium have been obtained by the OPW procedure and used to calculate the Knight shifts and relaxation times in beryllium and magnesium. The results provide an explanation of the small observed Knight shift in beryllium and the substantial Knight shift in magnesium. The small spin density obtained in beryllium explains the origin of the rather long relaxation time T_1 found experimentally. The relaxation time in magnesium on the other hand, was found to be about 25 times faster than that of beryllium, but much longer than that observed in aluminum. Our predicted long relaxation time in magnesium is consistent with the experimental observation[47] of substantial distortion of the resonance lines by saturation at 1.2°K.

An important result of general interest from these calculations is the observation that the cp due to the p component of the conduction-electron wave function is negative in beryllium and positive in magnesium. In both these cases, the inclusion of this effect improves the agreement between theoretical and experimental Knight shifts. Thus, in beryllium, it cancels a large part of the direct Knight shift and reduces the total to a small value. In magnesium, on the other hand, the cp effect adds to the direct Knight shift and again markedly improves the agreement. This feature of the cp effect also has an important influence on the Korringa constants in these metals. The differing signs of the cp effect in beryllium and magnesium indicate that one has to be cautious in making general assumptions regarding its sign in the interpretation of Knight shift data in pure metals and alloys.

The remaining difference between the theoretical and experimental Knight shifts is attributed in beryllium mainly to a negative Landau-type orbital effect. In magnesium, the difference between experiment and theory is expected to arise principally from the uncertainties in the Pauli spin susceptibility. However, other mechanisms such as core-conduction correlation and Van Vleck–Ramsey type orbital contribution to K_s could also provide improvements in the right direction. Experimental data on T_1 and spin susceptibility χ_p^*, when available, would be helpful for a better understanding of the relative importance of various contributing mechanisms to the hyperfine properties of magnesium.

Finally, we would like to draw attention once again to the dilemma of understanding the disagreement between the experimental and theoretical Pauli spin susceptibiltiy in beryllium. The experimental result for χ_p^* from spin-resonance measurements is expected to be quite accurate. The theoretical value from the calculated band density of states seems to require a strong deenhancement (about a factor of 3) to explain the observed χ_p^*, in contrast with the enhancement predicted by theoretical models. A much feebler deenhancement seems to be necessary to explain the experimental $(T_1T)^{-1}$. It appears, therefore, that further development of the theory for exchange and correlation effects for Bloch electrons in a magnetic field beyond current models is necessary before one can understand the uniform field susceptibility $\chi(0)$ and the wave-number–dependent susceptibility $\chi(\mathbf{q})$ that occurs in the theory of $(T_1T)^{-1}$.

ACKNOWLEDGMENTS

We would like to thank the computing center staff of the University of California for their kind help. One of us (S.D.M.) is grateful to Dr. Y. Yafet for helpful discussions. We would also like to thank Dr. D. L. Williams for sending a report prior to publication of Ref. 47.